

Supporting information

Effects of TiCl_4 Treatment on Structural and Electrochemical Properties of a Porous TiO_2 Layer in $\text{CH}_3\text{NH}_3\text{PbI}_3$ Perovskite Solar Cells

H. K. Adli^{a†}, T. Harada^{a,*}, S. Nakanishi^a and S. Ikeda^b

^a *Research Center for Solar Energy Chemistry, Osaka University, 1-3 Machikaneyama, Toyonaka, Osaka 560-8531, Japan.*

^b *Department of Chemistry, Faculty of Science and Engineering, Konan University Okamoto, Higashinada, Kobe 658-8501, Japan.*

[†] *Current affiliation: Faculty of Bioengineering and Technology, Universiti Malaysia Kelantan, Locked Bag No 100, Jeli, 17600, Kelantan, Malaysia.*

*Corresponding author: harada@chem.es.osaka-u.ac.jp

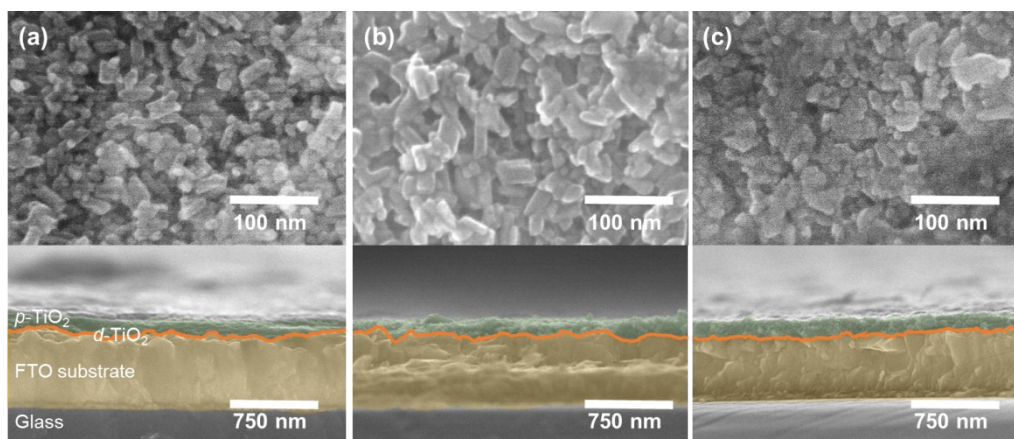


Figure S1. FE-SEM images of the surface morphology and cross section of (a) $p\text{TiO}_2(0)$, (b) $p\text{TiO}_2(50)$ and (c) $p\text{TiO}_2(100)$, respectively. SEM images were recorded at an acceleration voltage of 20 kV.

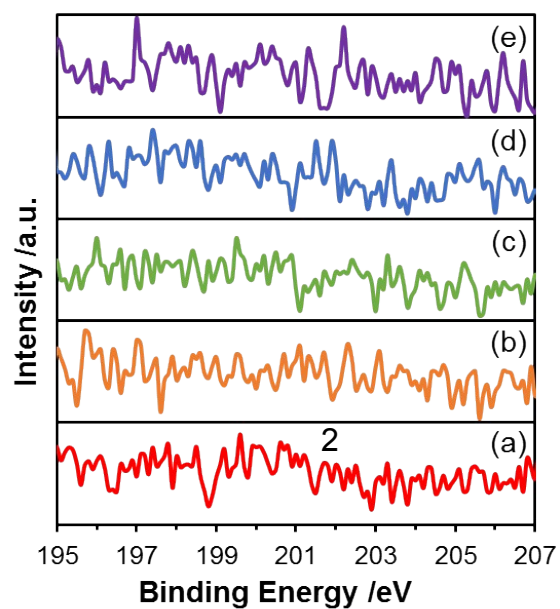


Figure S2. Cl 2p XPS of (a) $p\text{TiO}_2(0)$, (b) $p\text{TiO}_2(20)$, (c) $p\text{TiO}_2(50)$, (d) $p\text{TiO}_2(80)$ and (e) $p\text{TiO}_2(100)$.

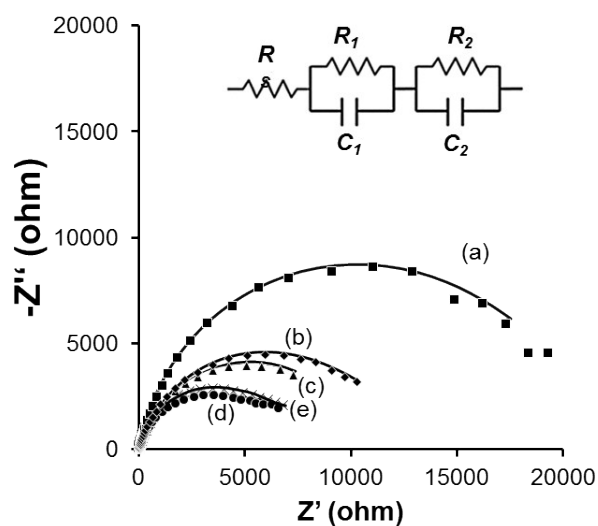


Figure S3 Nyquist plots of EIS measurements under 100 mW cm^{-2} illumination patterns of (a) $p\text{TiO}_2(0)$, (b) $p\text{TiO}_2(20)$, (c) $p\text{TiO}_2(50)$, (d) $p\text{TiO}_2(80)$ and (e) $p\text{TiO}_2(100)$. Inset shows the equivalent circuit model employed for fitting the Nyquist plot. R_s (ohmic series resistance), R_1 (charge transfer resistance of counter/electrolyte interface), C_1 (capacitance of counter/electrolyte interface), R_2 (charge transfer resistance of $p\text{TiO}_2$ /electrolyte interface) and C_2 (capacitance of $p\text{TiO}_2$ /electrolyte interface). For the analyses, constant phase elements were used instead of ideal capacitance in order to improve the quality of fittings.

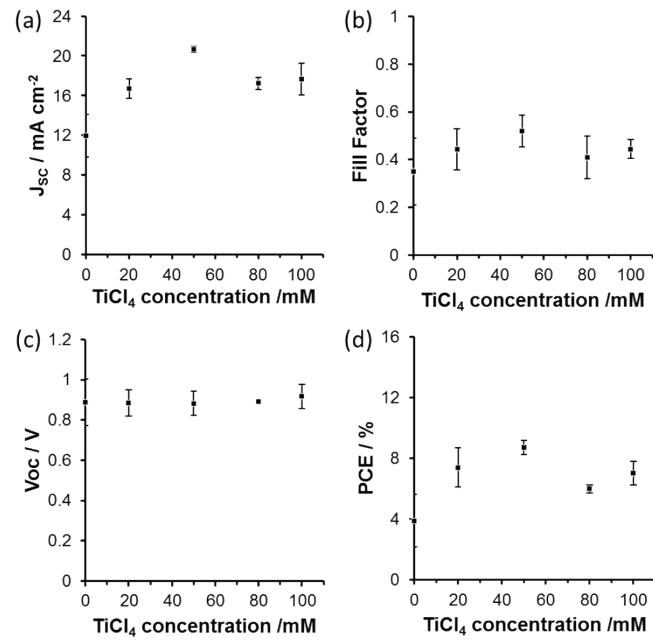


Figure S4 Photovoltaic performances of the $\text{CH}_3\text{NH}_3\text{PbI}_3$ perovskite solar cells deposited on $p\text{TiO}_2$ layer treated at different concentrations of TiCl_4 solution treatment for forward scan conditions; (a) short circuit current density (J_{sc}), (b) fill factor, (c) open circuit voltage (V_{oc}) and (d) power conversion efficiency (PCE). Each point represents the average value with standard deviation (error bars).

Table S1 Summary of electrochemical impedance parameters of various $p\text{TiO}_2$ samples

| | R_s / Ω | R_1 / Ω | R_2 / Ω |
|----------------------|----------------|------------------|------------------|
| $p\text{TiO}_2(0)$ | 27 | 61×10^2 | 19×10^3 |
| $p\text{TiO}_2(20)$ | 27 | 61×10^2 | 78×10^2 |
| $p\text{TiO}_2(50)$ | 43 | 54×10^2 | 54×10^2 |
| $p\text{TiO}_2(80)$ | 31 | 62×10^2 | 33×10^2 |
| $p\text{TiO}_2(100)$ | 29 | 55×10^2 | 41×10^2 |

Table S2 Summary of electrochemical impedance parameters of $\text{CH}_3\text{NH}_3\text{PbI}_3$ perovskite solar cells based on various $p\text{TiO}_2$ samples

| | R_s / Ω | R_{sc} / Ω | R_{rec} / Ω |
|----------------------|----------------|-------------------|--------------------|
| $p\text{TiO}_2(0)$ | 30 | 45×10^2 | 11×10^3 |
| $p\text{TiO}_2(20)$ | 14 | 42×10^1 | 50×10^2 |
| $p\text{TiO}_2(50)$ | 22 | 14×10^2 | 56×10^3 |
| $p\text{TiO}_2(80)$ | 20 | 27×10^2 | 40×10^3 |
| $p\text{TiO}_2(100)$ | 30 | 63×10^1 | 12×10^3 |